platform, correct the coordinates of each datum in the volume scan for the platform motion, relative to the initial time of the volume scan. In this way, the various product-making algorithms will be guaranteed access to the data at all times (i.e., the radar data will never be outside the grid bounds), and the data coordinates will all be normalized to a common time, which will satisfy the requirements of the NRL product algorithms provided that the evolution of the precipitation system is negligible for the brief duration of each volume scan.

3 Sample SPS-48E products from NRL-NOWCAST

On 18 January 2006 an occluded baroclinic wave traversed the north-east coast of the United States. Precipitation associated with the cold front of this wave was observed by the network of Weather Surveillance Radar-1988 Doppler (WSR-88D) units in the area, as well as by the land-based SPS-48E radar located at Dam Neck, Virginia. This section demonstrates NRL-NOWCAST image products generated from the full-volume, full-resolution radar data taken by the SPS-48E, and compares them with images obtained with WSR-88D units located at Dover AFB, New Jersey (KDOX) and Norfolk, Virginia (KAKQ). KDOX and KAKQ are located approximately 230 km north and 100 km east of the SPS-48E at Dam Neck, Virginia, respectively.

3.1 Composite reflectivity

Figure 1 shows the composite reflectivity product derived from KDOX, the SPS-48E and KAKQ radar data near 1206 and 1339 UTC. Note that the SPS-48E and KAKQ, which are showing the southern end of the gust front, have the most overlap and are most easily compared. The differences in echo intensity between the images near the same times can be explained by the relative positions of the radars and the corresponding altitudes observed by each radar elevation scan, and the shallowness of the precipitation cells that make up this weather system as confirmed by inspection of the individual elevation scans that contribute to the composite reflectivity images. All of these images clearly show a thin line of higher reflectivity associated with a gust front near the eastern edge of the weather system; however, this feature is actually most distinct and its eastward propagation most evident in the SPS-48E data.

3.2 Radial velocity

Figures 2-4 show the radial velocity derived from the lowest elevation scans of the SPS-48E, KAKQ and KDOX radar data near 1206 and 1339 UTC. The maximum unambiguous range for the SPS-48E (51.7 km) and the Nyquist velocity (59.5 m s^{-1}) are much smaller and larger, respectively, compared to those of the WSR-88D units. Therefore, there is much less data shown in Fig. 2 compared to Figs. 3-4 and there is more aliased radial velocities evident in the raw data of Figs. 3-4 compared to Fig. 2. The majority of the SPS-48E raw data are successfully de-aliased with only a few residual aliased data shown in the north-east section of Fig. 2b. The sharp wind shift associated with the gust front is seen in all three figures, and the wind shift associated with the cold front is visible as a discontinuity in the zero isodop at the shoreline, approximately 90 km west of the gust front in Fig. 4c-d.

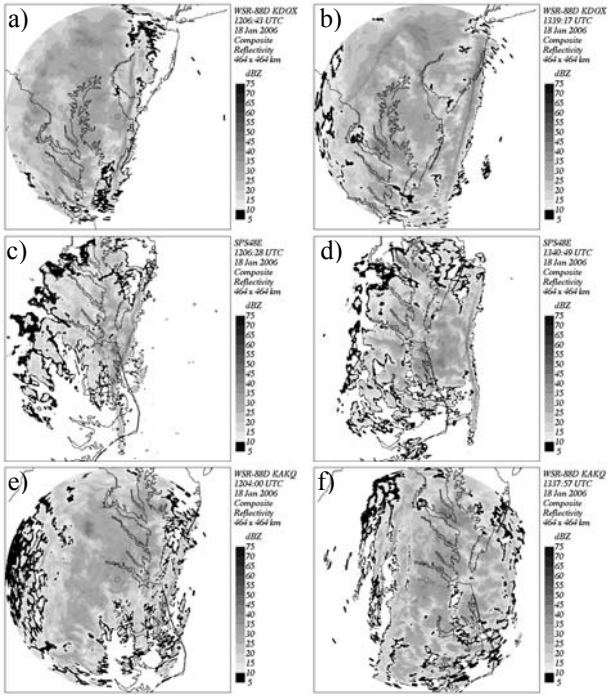

Fig. 1. Composite reflectivity near 1206 (left panel) and 1339 (right panel) UTC for a) and b) KDOX. c) and d) the SPS-48E, and e) and f) KAKQ.

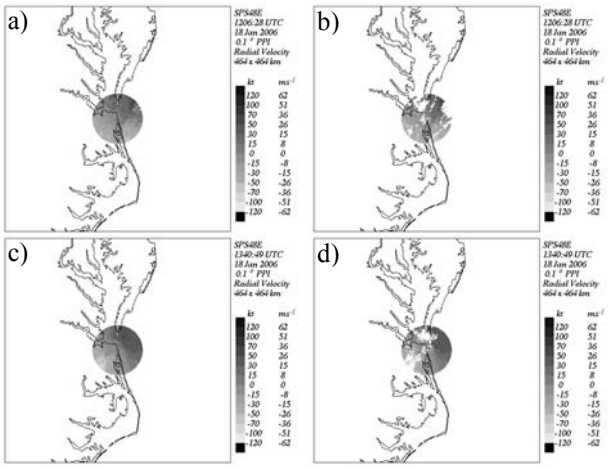

Fig. 2. Raw radial velocity (left panel) and quality controlled radial velocity (right panel) from the SPS-48E at a) and b) 1206 UTC and c) and d) 1340 UTC.

3.3 VAD winds

Figure 5 shows the Velocity Azimuth Display (VAD) method (Browning and Wexler 1968) winds derived from the KDOX, SPS-48E and KAKQ radar data near 1206 and 1339 UTC The VAD winds for the SPS-48E are only shown up to 4000 feet in these images because radial velocity data

are only available from the three lowest elevation scans of the SPS-48E volume scan. Nevertheless, such wind information would be invaluable to operators trying to avoid low level wind shear during aircraft operations around the ship. Despite the wind shift associated with the gust and cold fronts violating the linear wind assumptions required in the VAD method, all three radars provide reasonably consistent VAD wind estimates near the same times and altitudes.

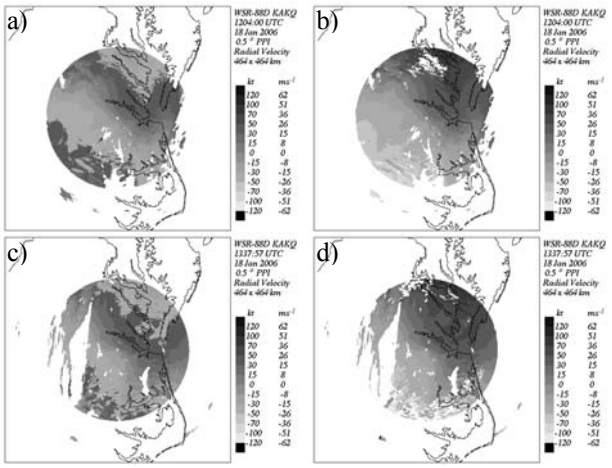

Fig. 3. Raw radial velocity (left panel) and quality controlled radial velocity (right panel) from KAKQ, at a) and b) 1204 UTC and c) and d) 1337 UTC.

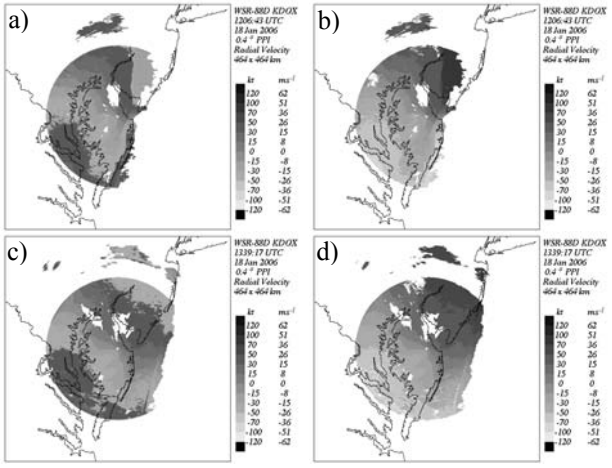

Fig. 4. Raw radial velocity (left panel) and quality controlled radial velocity (right panel) from KDOX, at a) and b) 1206 UTC and c) and d) 1339 UTC.

3.4 TITAN storm movement forecasts

A three-dimensional radar reflectivity mosaic algorithm was developed and applied to the volume scans from the SPS-48E and WSR-88D radars to create a single, combined data set at each time. The mosaic was then ingested into real-time tracking software that is used for producing short term (0-2 hour) forecasts of precipitation weather systems. The radar mosaic was ingested into the thunderstorm identification, tracking, analysis, and nowcasting (TITAN) software that can be used to extrapolate and trend existing areas of precipitation (delineated by a polygon representing a reflectivity threshold) out into the future. The software utilizes a sophisticated storm identification, analysis and tracking method that includes combinatorial optimization, and allowances for storm cell splits and mergers where applicable (Dixon and Weiner 1993).

Figure 6 shows the 30 minute TITAN forecasts of the 10 dBZ reflectivity contour of three storm cells at 1340 UTC; the main precipitation system associated with the cold front that includes the gust front, and two small storm cells at the western and southern edges of the main system. TITAN is able to accurately forecast the position of the first two storm cells, and only fails to forecast the merger of the southern cell with the main system, although the position of southern most half of this cell is reasonably well forecast.

4 Summary

The radar products shown in this paper have further verified the quality and accuracy of the SPS-48E radar data provided by the WEC and WDIC, and also demonstrate the readiness of NRL-NOWCAST to process SPS-48E data and extract valuable weather information from this data for operations.

Acknowledgements: The development of weather radar data quality control capability and NOWCAST system development are sponsored by the Office of Naval Research (ONR), PE 0602435N and PE 0602235N.

References

Browning, K. A., and R. Wexler, 1968: The determination of kinematic properties of a wind field using Doppler radar. *J. Appl. Meteor*., **7**, 105-113.

Cook, J., Q. Zhao, T. Tsui, P. Harasti and S. Potts, 2005: The Naval Research Laboratory NOWCAST system. *The World Weather Research Programme's Symposium on Nowcasting and Very Short Range Forecasting*, Toulouse, France, 5-9 September 2005, WWRP, EUMETSAT, AMS-Gematronik and Météo-France (available online at http://www.meteo.fr/cic/wsn05/DVD/index.html).

Dixon, M., and G. Wiener, 1993: TITAN: Thunderstorm identificaiton, tracking, analysis, and nowcasting – A radar-based methodology. J. Atmos. Oceanic Tech., **10**, 785-797.

Harasti, P. R., D. J. Smalley, M. E. Weber, C. Kessinger, Q. Xu, P. Zhang, S. Liu, T. Tsui, J. Cook, and Q. Zhao, 2005: On the development of a multi-algorithm radar data quality control system at the Naval Research Laboratory. *32nd Conference on Radar Meteorology*, Albuquerque, New Mexico, 24-28 October 2005, American Meteorological Society, 19pp (available at http://ams.confex.com/ams/32Rad11Meso/techprogram/session_18898.htm).

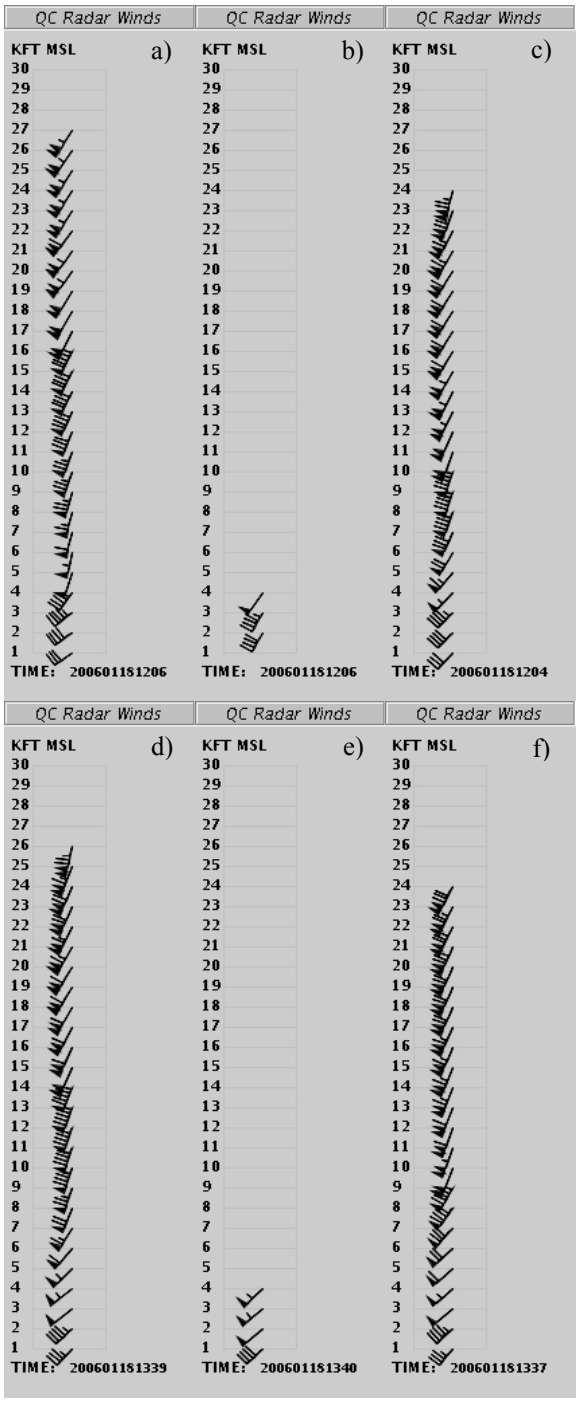

Fig. 5. Quality controlled VAD winds derived from radar data from a) and d) KDOX at 1206 and 1339 UTC, respectively, b) and e) the SPS-48E at 1206 and 1340 UTC, respectively, and c) and f) KAKQ at 1204 and 1337 UTC, respectively. 5000, 10,000 and 18,000 feet are approximately equivalent to 1.5, 3.0 and 5.0 km above mean sea level.

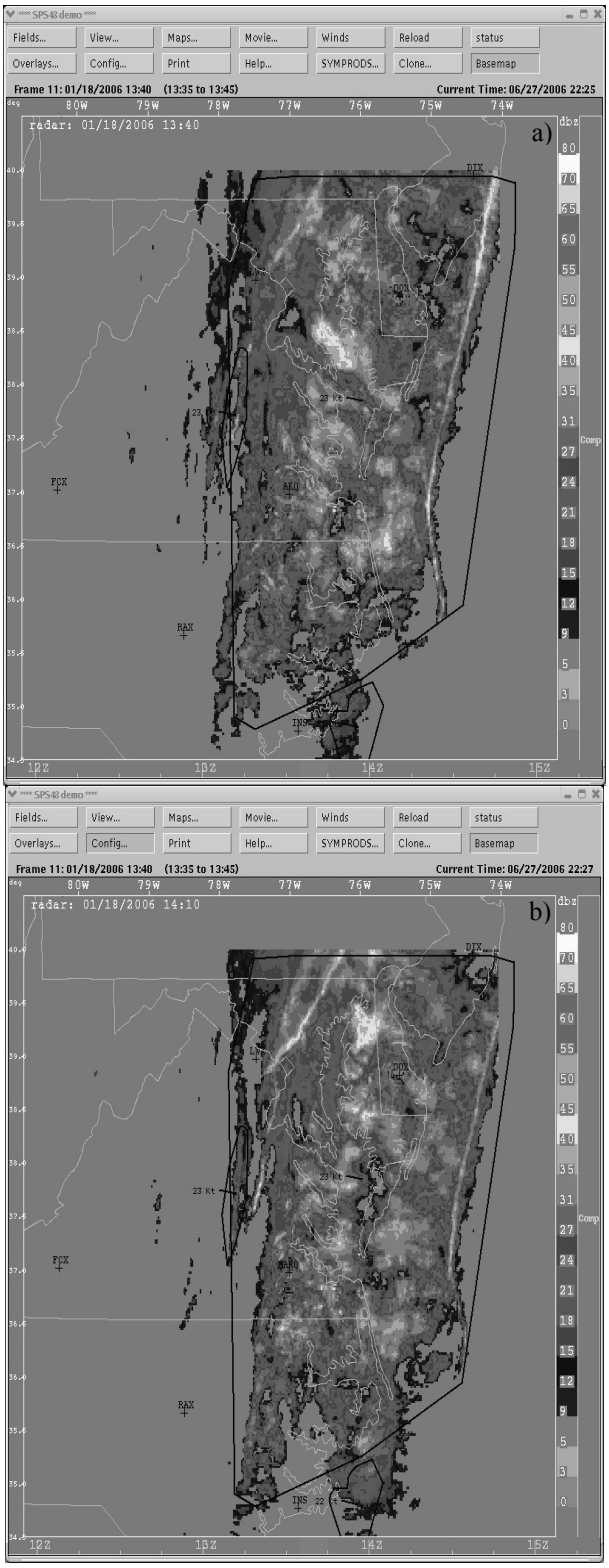

Fig. 6. Mosaic of composite reflectivity derived from the SPS-48E, KAKQ and KDOX reflectivity data at a) the TITAN forecast time of 1340 UTC, and b) the TITAN verification time of 1410 UTC. The three bold black polygons are the 30 minute TITAN forecasts of the 10 dBZ contour at 1340 UTC with the movement of the center of each polygon indicated by a bold black line with its speed given in kt.